European Journal of Radiology 138 (2021) 109676

Contents lists available at ScienceDirect

European Journal of Radiology

journal homepage: www.elsevier.com/locate/ejrad

Post-discharge chest CT findings and pulmonary function tests in severe COVID-19 patients

Maurizio Balbi [a,b,*], Caterina Conti [c], Gianluca Imeri [c], Anna Caroli [d], Alessandra Surace [a,b], Andrea Corsi [a,b], Elisa Mercanzin [a,b], Alberto Arrigoni [e], Giulia Villa [d], Fabiano Di Marco [c,f], Pietro Andrea Bonaffini [a,b], Sandro Sironi [a,b]

[a] Department of Radiology, ASST Papa Giovanni XXIII, Piazza OMS 1, Bergamo, BG, 24127, Italy
[b] Post Graduate School of Diagnostic Radiology, University of Milan-Bicocca, Piazza dell'Ateneo Nuovo 1, Milano, MI, 20126, Italy
[c] Respiratory Unit, ASST Papa Giovanni XXIII, Piazza OMS 1, Bergamo, BG, 24127, Italy
[d] Bioengineering Department, Istituto di Ricerche Farmacologiche Mario Negri IRCCS, Via Gian Battista Camozzi 3, Ranica, BG, 24020, Italy
[e] Department of Management, Information and Production Engineering, University of Bergamo, Via Pasubio 3, Dalmine, BG, 24044, Italy
[f] Department of Health Sciences, University of Milan, Via di Rudinì 8, Milano, MI, 20146, Italy

ARTICLE INFO

Keywords:
COVID-19
Severe acute respiratory syndrome coronavirus 2
Respiratory function tests
Tomography
Lung diseases
Survivors

ABSTRACT

Purpose: To evaluate chest computed tomography (CT) and pulmonary function test (PFT) findings in severe COVID-19 patients after discharge and correlate CT pulmonary involvement with PFT results.

Methods: COVID-19 patients admitted to our hospital between February 25 and May 2, 2020, were retrospectively included according to the following criteria: (a) COVID-19 defined as severe based on the WHO interim guidance (i.e., clinical signs of pneumonia plus respiratory rate > 30 breaths/min, severe respiratory distress, and/or SpO_2 < 90 % on room air); (b) chest radiograph in the acute setting; (c) post-discharge unenhanced chest CT; and (d) post-discharge comprehensive PFT. Imaging findings were retrospectively evaluated in consensus by two readers, and volume of abnormal lung was measured on CT using 3D Slicer software. Differences between demographics, comorbidities, acute radiographic findings, PFT, and post-discharge clinical and laboratory data of patients with normal and abnormal CT findings were assessed by Mann-Whitney or Fisher tests, and the compromised lung volume-PFT association by Pearson correlation after removing possible outliers.

Results: At a median of 105 days from symptom onset, 74/91 (81 %) patients had CT abnormalities. The most common CT pattern was combined ground-glass opacity and reticular pattern (46/74, 62 %) along with architectural distortion (68/74, 92 %) and bronchial dilatation (66/74, 89 %). Compromised lung volume had a median value of 15 % [11–23], was higher in dyspneic patients, and negatively correlated with the percentage of predicted DLCO, VA, and FVC values (r = -0.39, -0.5, and -0.42, respectively). These PFT parameters were significantly lower in patients with CT abnormalities. Impairment of DLCO and KCO was found in 12 (13 %) cases, possibly implying an underlying pulmonary vasculopathy in this subgroup of patients.

Conclusions: Most severe COVID-19 survivors still had physiologically relevant CT abnormalities about three months after the disease onset, with an impairment of diffusion capacity on PFT. A pulmonary vasculopathy was suggested in a minor proportion of patients.

1. Introduction

The severe acute respiratory syndrome coronavirus 2 is responsible for the coronavirus disease 2019 (COVID-19), an ongoing pandemic emergency that has affected more than 60 million people globally, with nearly 1.5 million deaths recorded by the World Health Organization

Abbreviations: COVID-19, coronavirus disease 2019; CT, computed tomography; CXR, chest radiograph; DLCO, diffusing capacity for carbon monoxide; FEV1, forced expiratory volume in the first second; FVC, forced vital capacity; GGO, ground-glass opacity; KCO, carbon monoxide transfer coefficient; mMRC, modified Medical Research Council; OP, organizing pneumonia; PFT, pulmonary function test; SARS, severe acute respiratory syndrome; VA, alveolar volume; WHO, World Health Organization.

* Corresponding author at: Department of Radiology, ASST Papa Giovanni XXIII, Piazza OMS 1, Bergamo, 24127, Italy.
E-mail address: balbi.m@libero.it (M. Balbi).

https://doi.org/10.1016/j.ejrad.2021.109676
Received 29 November 2020; Received in revised form 3 March 2021; Accepted 18 March 2021
Available online 20 March 2021

(WHO) as of November 29, 2020 [1]. The disease primarily involves the respiratory system and can lead to a broad spectrum of clinical manifestations, from asymptomatic carriage to respiratory failure and acute respiratory distress syndrome [2–4]. The most common indication for hospital admission is pneumonia, with the vast majority of patients being managed on general wards and a sizeable proportion requiring intensive care support [5].

Despite the increasing number of recoveries from COVID-19, there remain concerns about the long-term consequences following the initial illness. Studies investigating previous coronavirus outbreaks suggest that some of the COVID-19 survivors may experience long-term respiratory complications of the infection [6–9]. In a study of severe acute respiratory syndrome (SARS) survivors, 36 % and 30 % of the entire cohort still had physiologically relevant radiographic abnormalities three and six months after hospital discharge, respectively [6]. The most common pulmonary function tests' (PFT) abnormality was an impairment of diffusion capacity followed by reduced lung volume measurements [6]. Similarly, in survivors from Middle East respiratory syndrome, 36 % of patients had residual radiographic changes at a median follow-up of six weeks, mostly due to fibrosis [7]. Emerging data on COVID-19 further indicate that the disease can result in prolonged illness and persistent symptoms [10,11], with post-acute PFT and imaging findings that possibly imply a degree of pulmonary vasculopathy and interstitial lung involvement persisting in the recovery phase of the disease [12–15]. However, to the best of our knowledge, only a few studies have described computed tomography (CT) findings in discharged COVID-19 patients so far [15–17], and there are currently no data on the physiological relevance of chest CT abnormalities in COVID-19 survivors. Our study aimed (a) to describe the chest CT and PFT findings in a cohort of severe COVID-19 patients after discharge and (b) to correlate the extent of pulmonary involvement on CT with PFT results.

2. Materials and methods

The Institutional Review Board (Comitato Etico di Bergamo, Italy) approved this retrospective observational study and waived the need for written informed consent.

2.1. Study population and data collection

The study included consecutive discharged patients who had been admitted to our hospital (Papa Giovanni XXIII, Bergamo, Italy) between February 25 and May 2, 2020, due to COVID-19 pneumonia confirmed by a real-time reverse transcriptase-polymerase chain reaction. The inclusion criteria were as follows: (*a*) COVID-19 defined as severe based on the WHO interim guidance (i.e., clinical signs of pneumonia plus respiratory rate > 30 breaths/min, severe respiratory distress, and/or SpO_2 < 90 % on room air) [18], (*b*) chest radiograph (CXR) acquired in the acute phase of the disease at the emergency department presentation and/or during the hospital stay, (*c*) post-discharge unenhanced chest CT, and (d) post-discharge comprehensive PFT. The exclusion criteria were: (*a*) history of chronic pulmonary disease, (*b*) suboptimal PFT results (e.g., due to poor patient effort), and (*c*) low quality imaging data. Patients' demographics, smoking history, date of disease onset, disease severity, comorbidities, and post-discharge pulmonary evaluation report (including PFT, laboratory data, and symptoms) were extracted from electronic patient records. Follow-up duration was computed as time elapsed between disease onset and follow-up chest CT. Fig. 1 shows the study flow diagram.

2.2. CT image acquisition and analysis

Referral for post-discharge chest CT scan was based on clinical judgment, namely persistent symptoms and/or PFT abnormalities. Chest CT scans were acquired in the supine position at full inspiration, moving from the lung bases to the apex, with either a 64-slice or a 16-slice scanner (Brilliance 64 and MX 16-slice, respectively; Philips Medical Systems, Best, Netherlands). All CT acquisitions were performed without contrast medium and with the following parameters: tube voltage, 120–140 kVp; automatic exposure control for tube current; pitch, 0.6–1.2; collimation, 12−40 mm. Images were reconstructed with 0.9–1.5-mm slice thickness using sharp kernels and standard lung window settings (width, 1600 HU; level, -600 HU).

The CT images were evaluated in consensus by two reviewers (PAB, a radiologist with 10 years of experience; MB, a fourth-year radiology resident) blinded to clinical data. CT findings were defined in accordance with the Fleischner Society terminology and peer-reviewed literature on viral pneumonia [19,20]. For each CT scan, the reviewers were asked to visually assess the predominant pattern: ground-glass opacity (GGO), consolidation, or reticular pattern (consisting of reticulation, parenchymal bands, or subpleural curvilinear opacity without substantial GGO or consolidation). If no CT pattern could be clearly identified as predominant, the two most representative coexisting patterns were noted. In addition, the presence of bronchial dilatation (rather than bronchiectasis, to indicate that the damage might still be reversible), architectural distortion, cavitation, and pleural effusion were evaluated. The distribution of CT abnormalities was classified as follows: (*a*) peripheral (involving mainly the peripheral one-third of the lung), central (involving mainly the central two-thirds of the lung) or neither; (*b*) unilateral or bilateral; (*c*) predominantly upper (above the carina), middle (between the carina and the right inferior pulmonary vein), lower (below the right inferior pulmonary vein), or no zonal predominance. The pulmonary lobes involved were

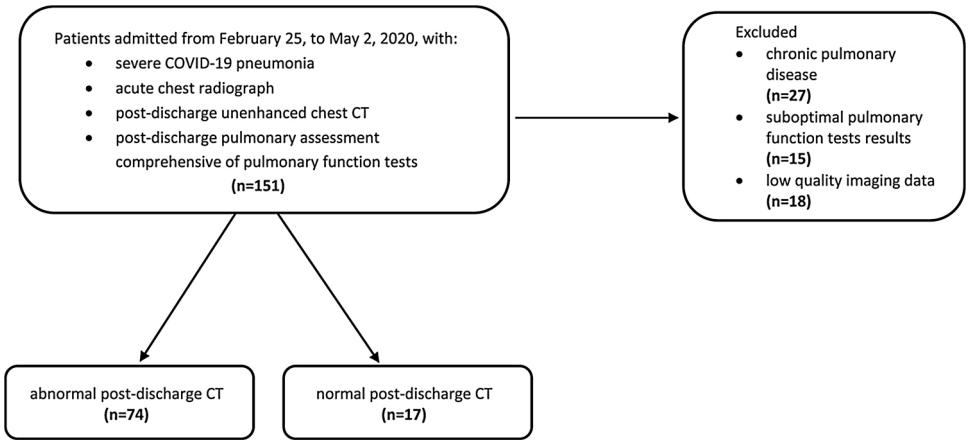

Fig. 1. Participant flow diagram.

also recorded.

The compromised lung volume was quantified using the open-source 3D Slicer software, version 4.8.1 (https://www.slicer.org). After denoising by median filtering ($1.5 \times 1.5 \times 1$ and $2 \times 2 \times 1$ kernel for CT scans acquired with the 64-slice and 16-slice scanner, respectively), lungs were automatically segmented using the Chest Imaging Platform extension (Applied Chest Imaging Laboratory, Boston, Massachusetts), also removing the central airways. Lung segmentations were eroded by 2 mm to account for possible partial volume effects, and remaining airways were further excluded through the Airway Segmentation Module and by imposing a -950 HU baseline minimum. Compromised lung was defined by image density over -800 HU, and the percentage of compromised lung over total lung volume was computed (Fig. 2). In case of unsatisfactory lung segmentation, the lung contours were manually edited.

2.3. CXR image acquisition and analysis

CXRs were obtained in the acute phase of the disease, namely at the emergency department presentation and/or during the hospital stay, using digital radiographic systems (Definium 8000, GE Healthcare, Milwaukee, USA; MOBILETT Elara Max, Siemens Healthineers, Erlangen, Germany), with tube voltage ranging from 70 to 150 kVp. The imaging data included CXR images acquired in the posteroanterior and lateral or anteroposterior projections. Only the anteroposterior and posteroanterior images were selected and retrospectively evaluated in consensus by two reviewers (PAB, a radiologist with 10 years of experience; MB, a fourth-year radiology resident) blinded to clinical data. The reviewers were asked to assess the presence of lung opacities (i.e., GGO, consolidation, or both) and grade each CXR using the *Brixia* score, an experimental 18-points severity scoring system designed for the assessment of COVID-19 pneumonia, as described in previous studies [21,22]. In addition, the overall extent of GGO and consolidation was assessed by visually estimating and then averaging the percentage of involvement within each lung. In case of multiple CXR, only the one showing the highest *Brixia* score was considered in the final analyses.

2.4. Post-discharge pulmonary assessment

Post-discharge pulmonary assessment included PFT, laboratory testing, and evaluation of symptoms.

PFT were performed according to current standards [23] by professionally trained respiratory technicians using Medical Graphics Elite Pro body box equipped with rapid gas analysers (MGC Diagnostics Corporation, USA) and interpreted by two experienced pulmonologists following current recommendations [24]. On account of COVID-19 restrictions, PFT were limited to spirometry and diffusing capacity for carbon monoxide (DLCO) [25]. Spirometric parameters comprised alveolar volume (VA), carbon monoxide transfer coefficient (KCO), forced vital capacity (FVC), forced expiratory volume in the first second (FEV1), and FEV1/FVC ratio. PFT parameters were expressed as a percent of the predicted value (%) and considered impaired if below the lower limit of normal according to the Global Lung Function Initiative 2012 reference equations for spirometry [26] and the Global Lung Function Initiative 2017 reference equations for DLCO [27]. The dyspnea intensity was evaluated using the modified Medical Research Council (mMRC) dyspnea scale.

2.5. Statistical analysis

Comparisons between patients with normal and abnormal chest CT were performed by Mann-Whitney or Fisher tests (numerical and binary/categorical variables, respectively). The strength of association between compromised lung volume and PFT results was assessed by Pearson correlation, after removing possible outliers. Overall and pairwise differences in compromised lung volume by the mMRC dyspnea scale score were assessed by Kruskal-Wallis and Wilcoxon test, respectively. Statistical significance was set at $p < 0.05$. All statistical analyses were performed using R software, version 3.6.3.

3. Results

Patients demographics, CXR findings, comorbidities, medical treatments (i.e., steroid and low molecular weight heparin), PFT results, and post-discharge clinical and laboratory data are reported in Table 1. The study finally included 91 patients (31 females, 34 %; median age 66 years, IQR = [59–73]). Most of them (78/91, 86 %) required oxygen supplementation for more than five days, while no patients were intubated nor admitted to the intensive care unit.

At a median of 105 days (IQR = [88–128]) after the disease onset, 74 (81 %) patients still had CT abnormalities. Most of them were male (53/74, 72 %) and significantly older ($p < 0.001$) than patients with a normal CT. No significant differences were found in comorbidities, while patients with an abnormal CT had more frequently received steroids during the hospital stay ($p = 0.031$). Consolidation frequency ($p = 0.001$), *Brixia* score ($p < 0.001$), and percentage of lung involvement ($p < 0.001$) on the acute CXR were found to be significantly higher in patients presenting with residual CT changes.

Post-discharge laboratory data did not significantly differ between the two groups of patients, except for higher D-dimer levels found in patients with CT abnormalities ($p < 0.001$). The most common symptoms were dyspnea (59/91, 65 %), asthenia (36/91, 40 %), and cough (16/91, 18 %), with no significant differences between patients with normal and abnormal CT.

A combination of GGO and the reticular pattern was the most common CT finding (46/74, 62 %) (Fig. 3), followed by reticular (17/74, 23 %) and GGO (10/74, 13 %) pattern. In the case of GGO predominance, GGO mostly showed a faint appearance (Fig. 4). The consolidation

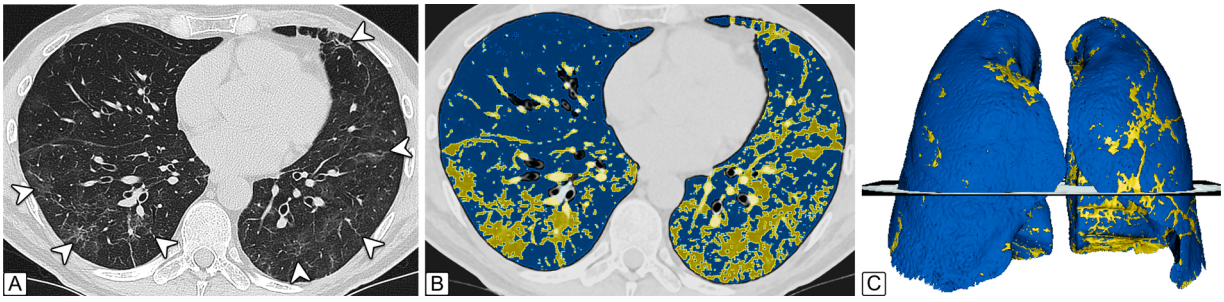

Fig. 2. Lung abnormality quantification on chest CT in a 61-year-old man who suffered severe COVID-19. (A) Unenhanced chest CT scan acquired 85 days after the disease onset shows residual bilateral lung abnormalities (white arrowheads). (B) The semiautomated segmentation performed by 3D Slicer software highlights the residual lung abnormalities (yellow) and normally aerated lung (blue). (C) 3D volumetric representation of both lungs illustrates the distribution of parenchymal abnormalities (yellow) and normally aerated lung (blue). The percentage of compromised lung volume was quantified as 20.7 %.

Table 1
Demographic, clinical, laboratory, and radiological findings in 91 COVID-19 survivors divided into groups based on post-discharge chest CT findings.

	All	CT+	CT-	p
Total no.	91	74	17	
Age, years	66 [59–73]	67 [61–74]	56 [49–66]	**<0.001**
Gender, F - no. (%)	31 (34)	21 (28)	10 (59)	**0.024**
Smoking history (Never/Former/Current), no. (%)	41(45)/50 (55)/0(0)	30(41)/44 (59)/0(0)	11(65)/6 (35)/0(0)	0.104
Follow-up duration, days	105 [88–128]	103 [88–126]	121 [86–136]	0.495
Chest X-ray findings during the acute illness				
Type of pulmonary opacity (GGO/GGO and consolidation), no. (%)	32(35)/59 (65)	20(27)/54 (73)	12(71)/5 (29)	**0.001**
Brixia score [21]	6 [4–8]	7 [5–9]	4 [3–4]	**<0.001**
% of lung involvement	30 [20–41]	34 [24–44]	15 [10–25]	**<0.001**
Laboratory data*				
D-dimer (ng/mL)	386 [240–618]	429 [283–716]	202 [190–342]	**<0.001**
CRP (mg/dL)	0.10 [0.10 – 0.40]	0.10 [0.10 – 0.40]	0.20 [0.05 – 0.30]	0.821
WBC (10^9/L)	6.44 [5.61–7.98]	6.49 [5.67–7.98]	6.22 [5.37–7.21]	0.536
Lymphocytes (WBC %)	32.9 [26.4–38.6]	33.2 [26.4–38.6]	30.4 [26.3–37.4]	0.702
Lymphocytes (10^9/L)	2.07 [1.53–2.70]	2.05 [1.52–2.72]	2.08 [1.53–2.52]	0.807
<1 – no./total no. (%)	5/86 (6)	4/70 (6)	1/16 (6)	1.000
Neutrophils (WBC %)	55.6 [48.4–62.0]	55.4 [48.0–61.8]	55.6 [51.1–64.0]	0.395
Neutrophils (10^9/L)	3.62 [2.96–4.44]	3.62 [2.95–4.42]	3.34 [3.03–4.51]	0.984
Symptoms*				
Asthenia	36 (40)	28 (38)	8 (47)	0.585
Dyspnea	59 (65)	50 (68)	9 (53)	0.272
mMRC dyspnea scale (0/1/2), no. (%)	25(27)/49 (54)/17(19)	18(24)/41 (56)/15(20)	7(41)/8 (47)/2(12)	0.444
Chest pain	5 (5)	3 (4)	2 (12)	0.233
Cough	16 (18)	14 (19)	2 (12)	0.727
Sputum	4 (4)	3 (4)	1 (6)	0.570
Comorbidities				
Any	69 (77)	59 (81)	10 (59)	0.064
>2	24 (27)	21 (29)	3 (18)	0.544
Arterial hypertension	48 (53)	42 (57)	6 (35)	0.177
Cardiovascular disease**	19 (21)	17 (23)	2 (12)	0.509
Obesity***	25 (27)	20 (27)	5 (29)	1.000
Diabetes	14 (2)	11 (15)	3 (18)	0.723
Dyslipidemia	29 (32)	25 (34)	4 (24)	0.567
Chronic renal failure	3 (3)	2 (3)	1 (6)	0.466
Neoplasia (active history)	3 (3)	3 (4)	0 (0)	1.000
Rheumatic pathology	5 (5)	5 (7)	0 (0)	0.579
Immunodepression	5 (5)	5 (7)	0 (0)	0.579
Epilepsy	1 (1)	1 (1)	0 (0)	1.000
Cirrhosis	1 (1)	0 (0)	1 (6)	0.187
Medical treatments				
Steroid				
During hospitalization	44 (48)	40 (54)	4 (24)	**0.031**
Current	1 (1)	1(1)	0(0)	1.000
LMWH				
During hospitalization	76 (84)	64 (86)	12 (71)	0.146
Current	7 (8)	6 (8)	1 (6)	1.000
Pulmonary function tests				
FVC % predicted	88 [79–99]	87 [79–96]	99 [90–109]	**0.016**
<LLN – no. (%)	16 (18)	13 (18)	3 (18)	1.000
FEV1 % predicted	90 [81–103]	90 [80–99]	102 [82–114]	0.096
<LLN – no. (%)	17 (19)	13 (18)	4 (24)	0.730
FEV1/FVC % predicted	104 [99–109]	104 [99–110]	103 [97–106]	0.158
<LLN – no. (%)	7 (8)	5 (7)	2 (12)	0.661
VA % predicted	89 [81–102]	88 [79–98]	108 [84–116]	**0.009**
<LLN – no. (%)	24 (26)	20 (27)	4 (24)	1.000
DLCO % predicted	81 [72–103]	79 [70–96]	103 [78–116]	**0.006**
<LLN – no. (%)	33 (36)	29 (39)	4 (24)	0.274
KCO % predicted	94 [83–101]	94 [82–101]	98 [90–114]	0.180
<LLN – no. (%)	12 (13)	11 (15)	1 (6)	0.452

Data are reported as median [IQR] (continuous/numerical variables) or number (%) (binary/categorical variables). p-values are computed between COVID-19 survivors with normal and abnormal chest CT (CT + and CT-, respectively) by Mann-Whitney test (continuous variables) or Fisher's exact test (binary or categorical variables). Abbreviations: GGO = ground-glass opacity, CRP = C-reactive protein, WBC = white blood cells, mMRC = modified Medical Research Council, FVC = forced vital capacity, FEV1 = forced expiratory volume in the first second, LLN = lower limit of normal, VA = alveolar volume, DLCO = diffusion capacity for carbon monoxide, KCO = carbon monoxide transfer coefficient, LMWH = low molecular weight heparin.

* At the time of post-discharge pulmonary evaluation.

** Including coronary heart disease, cerebrovascular disease, heart failure, and peripheral vascular disease.

*** Defined as BMI ≥ 30.

pattern was found only in one case and showed a perilobular distribution highly suggestive of organizing pneumonia (OP). Bronchial dilatation and architectural distortion (Fig. 5) coexisted in most patients (66/74, 89 %, and 68/74, 92 %, respectively). CT abnormalities were bilateral in 72/74 (97 %) cases, and in most cases did not show any zonal predominance (Table 2).

The most common PFT abnormalities were impaired DLCO (33/91, 36 %) and VA (24/91, 26 %). DLCO%, VA%, and FVC% were significantly lower in patients with CT abnormalities ($p = 0.006$, 0.009, and 0.016, respectively), while no differences were found for FEV1/FVC% ($p = 0.158$) and KCO% ($p = 0.180$). The latter was impaired in 12 (13 %) patients, all with impairment of DLCO, 11 with abnormal CT. The percentage of lung involvement on CT (median value = 15, IQR = [11–23]) was found to be higher in dyspneic patients and to show a significant negative correlation with DLCO% ($r = -0.39$, $p < 0.001$), VA% ($r = -0.5$, $p < 0.001$), and FVC% ($r = -0.42$, $p < 0.001$) (Fig. 6).

4. Discussion

With the intention of identifying and timely managing respiratory complications from COVID-19, current recommendations state that patients who suffered severe COVID-19 pneumonia should undergo a clinical and radiological assessment 12 weeks after discharge [28]. In the present study, a significant proportion of such patients still had physiologically relevant CT abnormalities even beyond that time point, further highlighting the need for follow-up strategies to support COVID-19 survivors through the recovery phase. The most common CT findings were GGO admixed with reticulation and linear opacities (i.e., parenchymal bands and subpleural curvilinear lines), along with signs of architectural distortion and bronchial dilatation. The percentage of lung involvement correlated with PFT findings and dyspnea severity.

CT abnormalities were consistent with previous studies describing GGO as a common persistent finding, a progressive increase in linear and reticular opacities during illness, and the frequency of consolidation considerably diminishing after the acute phase of the disease [20,29]. These findings seem to mirror organization, with parenchymal bands possibly indicating OP or atelectasis, while reticulation combined with architectural distortion suggesting a progression to fibrosis [30–32]. In cases where GGO and reticulation predominantly involved basal lungs,

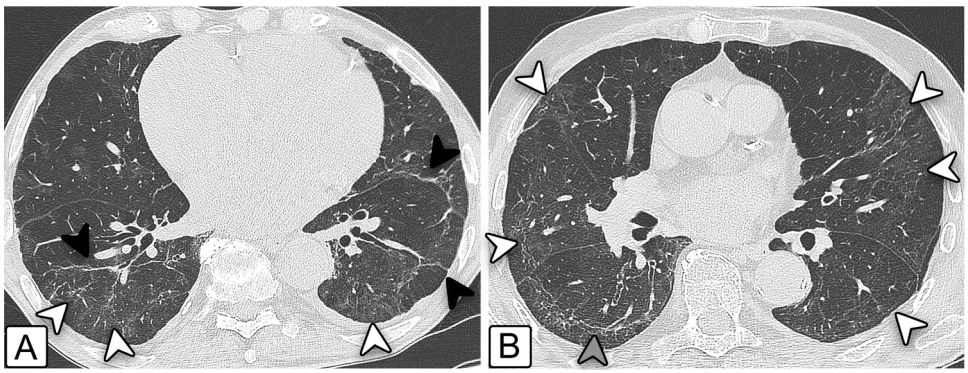

Fig. 3. Images from unenhanced chest CT scan of an 89-year-old man who suffered severe COVID-19. The examination was performed 96 days after the disease onset. Axial images show bilateral ground-glass opacity with superimposed reticulation (white arrowheads, A and B), parenchymal bands (black arrowheads, A) and subpleural curvilinear opacities (gray arrowhead, B).

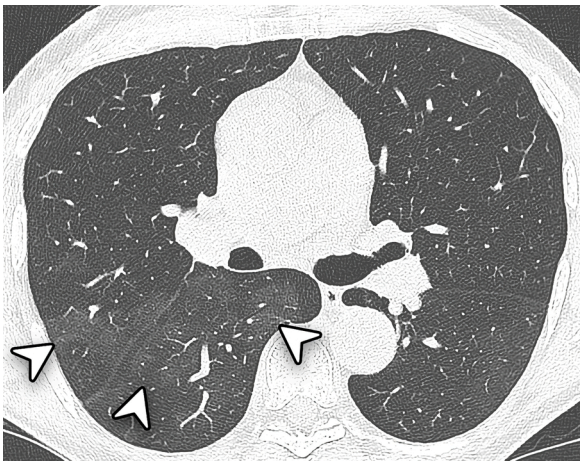

Fig. 4. Unenhanced chest CT scan of a 58-year-old man who suffered severe COVID-19. The examination was performed 88 days after the disease onset. Axial image shows pure faint ground-glass opacity in the right upper and lower lobes (white arrowheads).

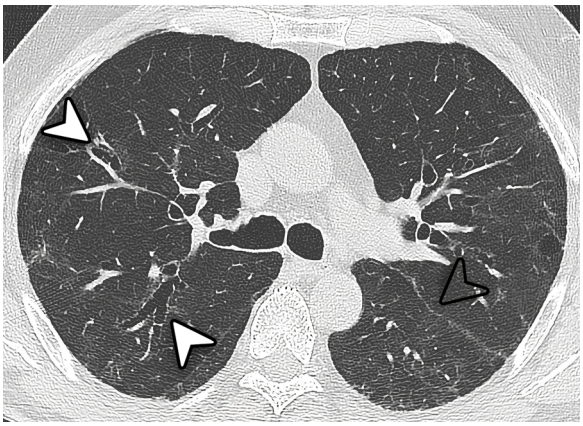

Fig. 5. Unenhanced chest CT scan of an 82-year-old man who suffered severe COVID-19. The examination was performed 98 days after the disease onset. Axial image shows central bronchial dilatations (white arrowheads) and scissural distortion (empty arrowhead). Reticulation coexisted in both lungs.

the pattern of lung abnormalities resembled that of non-specific interstitial pneumonia (Fig. 7), which has been pointed out as a potential sequela of OP in some instances [33]. Interestingly, pure faint GGO was observed only in a small percentage of patients, especially in those with

Table 2
Post-discharge CT findings in 74 COVID-19 survivors.

% of compromised lung volume	15 [11–23]
Type of CT pattern	
GGO	10 (13)
Reticular	17 (23)
Combined GGO and reticular	46 (62)
Consolidation	1 (1)
Architectural distortion	68 (92)
Bronchial dilatation	66 (89)
Emphysema	7 (9)
Cavitation	1(1)
Pleural effusion	1 (1)
Distribution	
Bilateral	72 (97)
Axial distribution (central/peripheral/neither)	1(1)/25(34)/48(65)
Cranio-caudal distribution (superior/medium/inferior/none)	3(4)/1(1)/14(19)/56 (76)
RUL	71 (96)
ML	68 (92)
RLL	70 (95)
LUL	62 (84)
Lingula	66 (89)
LLL	69 (93)

Data are reported as median [IQR] (continuous/numerical variables) or number (%) (binary/categorical variables). Abbreviations: GGO = ground-glass opacity, RUL = right upper lobe, ML = middle lobe, RLL = right lower lobe, LUL = left upper lobe, LLL = left lower lobe.

a lower peak radiographic involvement, possibly indicating a late recovery stage in relatively less severe cases. Nevertheless, the underlying pathologic processes of residual CT abnormalities in COVID-19 survivors remain speculative, and whether such lung's responses to injury will heal without permanent damage or turn out to be a pathway to fibrosis remains to be further investigated.

We found CT abnormalities to be physiologically relevant and their extent to be indicative of respiratory impairment. In keeping with previous studies investigating SARS survivors [6,9], DLCO was the most frequently impaired PFT parameter, followed by a reduction in VA and FVC, while impaired KCO was less common. DLCO gives an overall assessment of the lung's ability of gas exchange and may occur with various combinations of KCO and VA, each suggesting different underlying pathologies. Decreased KCO occurs in alveolar-capillary damage, microvascular pathology, or anemia, while causes of low VA include reduced alveolar expansion, alveolar damage or loss, or ventilation/perfusion mismatch as seen in airflow obstruction [34]. DLCO, VA, and FVC were significantly lower in patients with an abnormal CT and consistent with imaging findings, indicating an impairment of diffusion capacity and a tendency toward restrictive physiology due to post-inflammatory changes as the most frequent abnormalities. Notably,

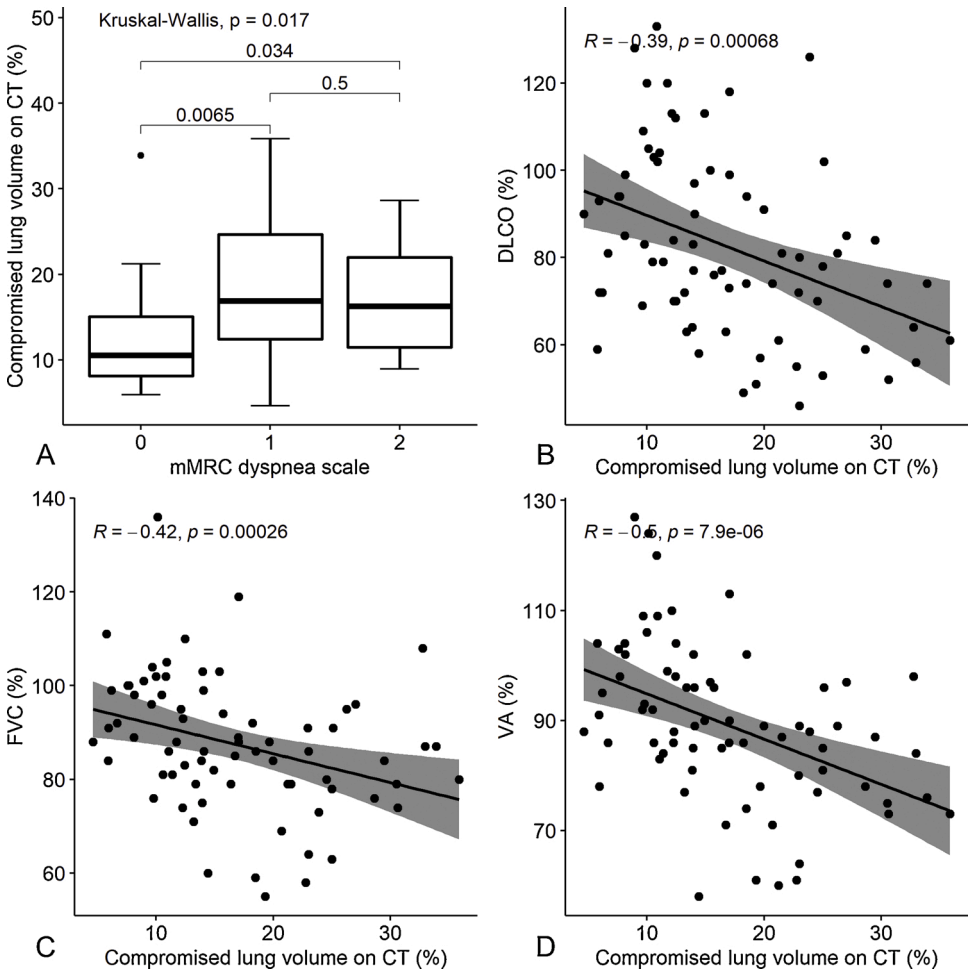

Fig. 6. Associations between pulmonary involvement on CT and dyspnea intensity and pulmonary function test findings in 74 COVID-19 survivors. (A) Distribution of compromised lung volume on CT by the mMRC dyspnea score: *p* values denote significance in overall and pairwise differences assessed by Kruskal-Wallis and Wilcoxon test, respectively. (B-D) Linear regression of compromised lung volume on DLCO, FVC, and VA % predicted. R denotes Pearson's correlation coefficient, with the pertinent p-value. Abbreviations: mMRC = modified Medical Research Council, DLCO = diffusion capacity for carbon monoxide, FVC = forced vital capacity, VA = alveolar volume.

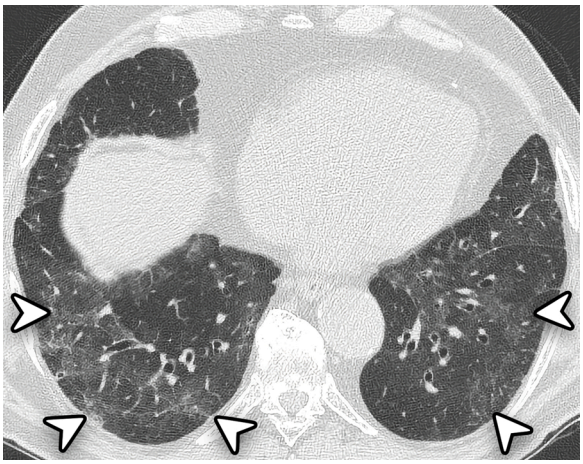

Fig. 7. Unenhanced chest CT scan of a 59-year-old man who suffered severe COVID-19. The examination was performed 84 days after the disease onset. Axial image shows lower lobe predominant ground-glass opacity admixed with reticulation (white arrowheads) and relative sparing of the subpleural lung, suggesting a non-specific interstitial pneumonia pattern.

a minor proportion of patients had an impairment of DLCO and KCO, suggesting membrane lesion rather than reduced lung volume as the main cause of impaired diffusion capacity in these cases. Endothelial dysfunction and thrombosis are factors contributing to the pathogenesis of COVID-19 [35–39], hence the interest of pulmonary perfusion assessment techniques, such as dual-energy CT, for the evaluation of COVID-19 survivors [40,41].

Current results are in line with a previous study investigating SARS outpatients [42], where a greater peak of radiographic opacification in the acute phase of the disease was associated with a higher risk of developing pulmonary sequelae on CT. Moreover, we found residual imaging abnormalities to be significantly more frequent in older patients and men, suggesting that such groups of survivors may show a relatively slower resolution rate and potentially worse outcomes. These results are consistent with previous studies that reported increasing age and male sex as high-risk factors for a worse disease course in patients suffering from COVID-19 [43,44].

The present study has some limitations. First, selection bias may have occurred due to the retrospective nature of the study design. Moreover, a larger sample size, longer follow-up period, and baseline CT examination are needed to depict the full spectrum of the disease course. Also, though having excluded patients known for chronic respiratory disease enables assuming that baseline lung function was normal in most patients, the lack of PFT prior to the disease onset prevented from comparing pre- and post-disease pulmonary function status. Lastly, lung volumes by whole-body plethysmography were not assessed.

In conclusion, we found a considerable proportion of severe COVID-19 survivors still having physiologically relevant CT abnormalities, even beyond three months after the disease onset. The percentage of lung involvement on CT correlated with dyspnea severity and PFT, with the latter suggesting an impairment of diffusion capacity and a tendency toward restrictive physiology as the most frequent abnormalities. An underlying pulmonary vasculopathy was suggested in a minor but not negligible proportion of patients. Further studies are needed to assess

the longitudinal evolution of imaging and functional pulmonary abnormalities in COVID-19 survivors.

Funding

None.

CRediT authorship contribution statement

Maurizio Balbi: Conceptualization, Methodology, Investigation, Data curation, Writing - original draft, Writing - review & editing, Visualization. **Caterina Conti:** Methodology, Investigation, Data curation, Writing - original draft, Writing - review & editing. **Gianluca Imeri:** Methodology, Investigation, Data curation, Writing - original draft, Writing - review & editing. **Anna Caroli:** Methodology, Formal analysis, Investigation, Data curation, Writing - original draft, Writing - review & editing, Resources, Visualization. **Alessandra Surace:** Methodology, Investigation, Data curation. **Andrea Corsi:** Investigation, Data curation, Visualization. **Elisa Mercanzin:** Investigation, Data curation. **Alberto Arrigoni:** Formal analysis, Investigation, Data curation, Visualization. **Giulia Villa:** Formal analysis, Investigation, Data curation, Visualization. **Fabiano Di Marco:** Writing - review & editing, Supervision. **Pietro Andrea Bonaffini:** Investigation, Data curation, Writing - review & editing. **Sandro Sironi:** Writing - review & editing, Supervision.

Declaration of Competing Interest

The authors declare no conflict of interest.

References

[1] World Health Organization, WHO Coronavirus Disease (COVID-19) Dashboard, 2020. Published on November 29, https://covid19.who.int.
[2] W. Guan, Z. Ni, Y. Hu, W. Liang, C. Ou, J. He, L. Liu, H. Shan, C. Lei, D.S.C. Hui, B. Du, L. Li, G. Zeng, K.-Y. Yuen, R. Chen, C. Tang, T. Wang, P. Chen, J. Xiang, N. Zhong, Clinical characteristics of coronavirus disease 2019 in China, N. Engl. J. Med. 382 (18) (2020) 1708–1720, https://doi.org/10.1056/NEJMoa2002032.
[3] X. Yang, Y. Yu, J. Xu, H. Shu, J. Xia, H. Liu, Y. Wu, L. Zhang, Z. Yu, M. Fang, T. Yu, Y. Wang, S. Pan, X. Zou, S. Yuan, Y. Shang, Clinical course and outcomes of critically ill patients with SARS-CoV-2 pneumonia in Wuhan, China: a single-centered, retrospective, observational study, Lancet Respir. Med. 8 (5) (2020) 475–481, https://doi.org/10.1016/S2213-2600(20)30079-5.
[4] P. Mehta, D.F. McAuley, M. Brown, E. Sanchez, R.S. Tattersall, J.J. Manson, COVID-19: consider cytokine storm syndromes and immunosuppression, Lancet 395 (10229) (2020) 1033–1034, https://doi.org/10.1016/S0140-6736(20)30628-0.
[5] A.B. Docherty, E.M. Harrison, C.A. Green, H.E. Hardwick, R. Pius, L. Norman, K. A. Holden, J.M. Read, F. Dondelinger, G. Carson, L. Merson, J. Lee, D. Plotkin, L. Sigfrid, S. Halpin, C. Jackson, C. Gamble, P.W. Horby, J.S. Nguyen-Van-Tam, M. G. Semple, Features of 20 133 UK patients in hospital with covid-19 using the ISARIC WHO Clinical Characterization Protocol: prospective observational cohort study, BMJ. m 1985 (2020), https://doi.org/10.1136/bmj.m1985.
[6] D.S. Hui, Impact of severe acute respiratory syndrome (SARS) on pulmonary function, functional capacity and quality of life in a cohort of survivors, Thorax 60 (5) (2005) 401–409, https://doi.org/10.1136/thx.2004.030205.
[7] K.M. Das, E.Y. Lee, R. Singh, M.A. Enani, K. Al Dossari, K. Van Gorkom, S. G. Larsson, R.D. Langer, Follow-up chest radiographic findings in patients with MERS-CoV after recovery, Indian J. Radiol. Imaging 27 (July-September 3) (2017) 342–349, https://doi.org/10.4103/ijri.IJRI_469_16.
[8] L. Xie, Y. Liu, Y. Xiao, Q. Tian, B. Fan, H. Zhao, W. Chen, Follow-up study on pulmonary function and lung radiographic changes in rehabilitating severe acute respiratory syndrome patients after discharge, Chest 127 (6) (2005) 2119–2124, https://doi.org/10.1378/chest.127.6.2119.
[9] C.K. Ng, Six month radiological and physiological outcomes in severe acute respiratory syndrome (SARS) survivors, Thorax 59 (10) (2004) 889–891, https://doi.org/10.1136/thx.2004.023762.
[10] M.W. Tenforde, S.S. Kim, C.J. Lindsell, E. Billig Rose, N.I. Shapiro, D.C. Files, K. W. Gibbs, H.L. Erickson, J.S. Steingrub, H.A. Smithline, M.N. Gong, M.S. Aboodi, M.C. Exline, D.J. Henning, J.G. Wilson, A. Khan, N. Qadir, S.M. Brown, I.D. Peltan, M.J. Wu, Symptom duration and risk factors for delayed return to usual health among outpatients with COVID-19 in a multistate health care systems network—united States, March–june 2020, MMWR Morb. Mortal. Wkly. Rep. 69 (30) (2020) 993–998, https://doi.org/10.15585/mmwr.mm6930e1.
[11] A. Carfì, R. Bernabei, F. Landi & for the Gemelli Against COVID-19 Post-Acute Care Study Group. Persistent Symptoms in Patients After Acute COVID-19, JAMA 324 (6) (2020) 603, https://doi.org/10.1001/jama.2020.12603.
[12] R. Chen, Y. Gao, M. Chen, W. Jian, C. Lei, J. Zheng, S. Li, Impaired pulmonary function in discharged patients with COVID-19: more work ahead, Eur Resp J 56 (1) (2020), 2002194, https://doi.org/10.1183/13993003.02194-2020.
[13] X. Mo, W. Jian, Z. Su, M. Chen, H. Peng, P. Peng, C. Lei, R. Chen, N. Zhong, S. Li, Abnormal pulmonary function in COVID-19 patients at time of hospital discharge, Eur Resp J 55 (6) (2020), 2001217, https://doi.org/10.1183/13993003.01217-2020.
[14] G. Patelli, S. Paganoni, F. Besana, F. Codazzi, M. Ronzoni, S. Manini, A. Remuzzi, Preliminary detection of lung hypoperfusion in discharged Covid-19 patients during recovery, Eur J Rad 129 (2020), 109121, https://doi.org/10.1016/j.ejrad.2020.109121.
[15] Y. Huang, C. Tan, J. Wu, M. Chen, Z. Wang, L. Luo, X. Zhou, X. Liu, X. Huang, S. Yuan, C. Chen, F. Gao, J. Huang, H. Shan, J. Liu, Impact of coronavirus disease 2019 on pulmonary function in early convalescence phase, Respir. Res. 21 (1) (2020) 163, https://doi.org/10.1186/s12931-020-01429-6.
[16] D. Liu, W. Zhang, F. Pan, L. Li, L. Yang, D. Zheng, J. Wang, B. Liang, The pulmonary sequalae in discharged patients with COVID-19: a short-term observational study, Respir. Res. 21 (1) (2020) 125, https://doi.org/10.1186/s12931-020-01385-1.
[17] M. Yu, Y. Liu, D. Xu, R. Zhang, L. Lan, H. Xu, Prediction of the development of pulmonary fibrosis using serial thin-section CT and clinical features in patients discharged after treatment for COVID-19 pneumonia, Korean J. Radiol. 21 (6) (2020) 746, https://doi.org/10.3348/kjr.2020.0215.
[18] World Health Organization, Clinical Management of COVID-19: Interim Guidance, 27 May 2020, World Health Organization, 2020, https://apps.who.int/iris/handle/10665/332196.
[19] D.M. Hansell, A.A. Bankier, H. MacMahon, T.C. McLoud, N.L. Müller, J. Remy, Fleischner society: glossary of terms for thoracic imaging, Radiology 246 (3) (2008) 697–722, https://doi.org/10.1148/radiol.2462070712.
[20] Y. Wang, C. Dong, Y. Hu, C. Li, Q. Ren, X. Zhang, H. Shi, M. Zhou, Temporal changes of CT findings in 90 patients with COVID-19 pneumonia: a longitudinal study, Radiology 296 (2) (2020) E55–E64, https://doi.org/10.1148/radiol.2020200843.
[21] A. Borghesi, R. Maroldi, COVID-19 outbreak in Italy: experimental chest X-ray scoring system for quantifying and monitoring disease progression, Radiol. Med. 125 (5) (2020) 509–513, https://doi.org/10.1007/s11547-020-01200-3, era 20.
[22] M. Balbi, A. Caroli, A. Corsi, G. Milanese, A. Surace, F. Di Marco, L. Novelli, M. Silva, F.L. Lorini, A. Duca, R. Cosentini, N. Sverzellati, P.A. Bonaffini, S. Sironi, Chest X-ray for predicting mortality and the need for ventilatory support in COVID-19 patients presenting to the emergency department, Eur. Radiol. (2020), https://doi.org/10.1007/s00330-020-07270-1.
[23] B.L. Graham, I. Steenbruggen, M.R. Miller, I.Z. Barjaktarevic, B.G. Cooper, G. L. Hall, T.S. Hallstrand, D.A. Kaminsky, K. McCarthy, M.C. McCormack, C. E. Oropez, M. Rosenfeld, S. Stanojevic, M.P. Swanney, B.R. Thompson, Standardization of spirometry 2019 update. An Official American Thoracic Society and European Respiratory Society technical statement, Am. J. Respir. Crit. Care Med. 200 (8) (2019) e70–e88, https://doi.org/10.1164/rccm.201908-1590ST.
[24] R. Pellegrino, G. Viegi, V. Brusasco, R.O. Crapo, F. Burgos, R. Casaburi, A. Coates, C.P. van der Grinten, P. Gustafsson, J. Hankinson, R. Jensen, D.C. Johnson, N. MacIntyre, R. McKay, M.R. Miller, D. Navajas, O.F. Pedersen, J. Wanger, Interpretative strategies for lung function tests, Eur. Respir. J. 26 (5) (2005) 948–968, https://doi.org/10.1183/09031936.05.00035205.
[25] A. McGowan, K. Sylvester, F. Burgos, P. Boros, F. de Jongh, A. Kendrick, J. Lloyd Cooper, J. Kirkby, J. Makonga-Braaskma, I. Steenbruggen, J. den Berg, ERS 9.1 Statement on lung function during COVID-19 Final with Contributors, Ers (2020) 1–5. Accessed August 2, 2020, https://ers.app.box.com/s/zs1uu88wy51monr0ewd990itoz4tsn2h.
[26] P.H. Quanjer, S. Stanojevic, T.J. Cole, X. Baur, G.L. Hall, B.H. Culver, P.L. Enright, J.L. Hankinson, M.S. Ip, J. Zheng, J. Stocks, ERS Global Lung Function Initiative. Multi-ethnic reference values for spirometry for the 3-95-yr age range: the global lung function 2012 equations, Eur. Respir. J. 40 (6) (2012) 1324–1343, https://doi.org/10.1183/09031936.00080312.
[27] S. Stanojevic, B.L. Graham, B.G. Cooper, B.R. Thompson, K.W. Carter, R. W. Francis, G.L. Hall, Global Lung Function Initiative TLCO working group; Global Lung Function Initiative (GLI) TLCO. Official ERS technical standards: Global Lung Function Initiative reference values for the carbon monoxide transfer factor for Caucasians, Eur. Respir. J. 50 (September 3) (2017), 1700010, https://doi.org/10.1183/13993003.00010-2017.
[28] P.M. George, S.L. Barratt, R. Condliffe, S.R. Desai, A. Devaraj, I. Forrest, M. A. Gibbons, N. Hart, R.G. Jenkins, D.F. McAuley, B.V. Patel, E. Thwaite, L. G. Spencer, Respiratory follow-up of patients with COVID-19 pneumonia, Thorax 75 (11) (2020) 1009–1016, https://doi.org/10.1136/thoraxjnl-2020-215314.
[29] F. Pan, T. Ye, P. Sun, S. Gui, B. Liang, L. Li, D. Zheng, J. Wang, R.L. Hesketh, L. Yang, C. Zheng, Time course of lung changes at chest CT during recovery from coronavirus disease 2019 (COVID-19), Radiology 295 (3) (2020) 715–721, https://doi.org/10.1148/radiol.2020200370.
[30] S.J. Kligerman, T.J. Franks, J.R. Galvin, From the radiologic pathology archives: organization and fibrosis as a response to lung injury in diffuse alveolar damage, organizing pneumonia, and acute fibrinous and organizing pneumonia, Radiographics 33 (7) (2013) 1951–1975, https://doi.org/10.1148/rg.337130057.
[31] M. Zare Mehrjardi, S. Kahkouee, M. Pourabdollah, Radio-pathological correlation of organising pneumonia (OP): a pictorial review, Br. J. Radiol. (2017), 20160723, https://doi.org/10.1259/bjr.20160723.

[32] R. Polverosi, M. Maffessanti, G. Dalpiaz, Organizing pneumonia: typical and atypical HRCT patterns, Radiol. Med. 111 (2) (2006) 202–212, https://doi.org/10.1007/s11547-006-0021-8.
[33] J.W. Lee, K.S. Lee, H.Y. Lee, M.P. Chung, C.A. Yi, T.S. Kim, M.J. Chung, Cryptogenic organizing pneumonia: serial high-resolution CT findings in 22 patients, Am J Roentgenol 195 (4) (2010) 916–922, https://doi.org/10.2214/AJR.09.3940.
[34] J.M. Hughes, N.B. Pride, In defence of the carbon monoxide transfer coefficient Kco (TL/VA), Eur. Respir. J. 17 (2) (2001) 168–174, https://doi.org/10.1183/09031936.01.17201680.
[35] A.J. Kucharski, T.W. Russell, C. Diamond, Y. Liu, J. Edmunds, S. Funk, R.M. Eggo, F. Sun, M. Jit, J.D. Munday, N. Davies, A. Gimma, K. van Zandvoort, H. Gibbs, J. Hellewell, C.I. Jarvis, S. Clifford, B.J. Quilty, N.I. Bosse, S. Flasche, Early dynamics of transmission and control of COVID-19: a mathematical modelling study, Lancet Infect. Dis. 20 (5) (2020) 553–558, https://doi.org/10.1016/S1473-3099(20)30144-4.
[36] B.M. Henry, J. Vikse, S. Benoit, E.J. Favaloro, G. Lippi, Hyperinflammation and derangement of renin-angiotensin-aldosterone system in COVID-19: a novel hypothesis for clinically suspected hypercoagulopathy and microvascular immunothrombosis, Clin. Chim. Acta 507 (2020) 167–173, https://doi.org/10.1016/j.cca.2020.04.027.
[37] A.M. Ierardi, S.A. Angileri, A. Arrichiello, L. Di Meglio, M. Gurgitano, G.M. Rodà, G, Pulmonary embolism in COVID-19: ventilation and perfusion computed tomography, IDCases 21 (2020) (2020), e00805, https://doi.org/10.1016/j.idcr.2020.e00805.
[38] Z. Varga, A.J. Flammer, P. Steiger, M. Haberecker, R. Andermatt, A.S. Zinkernagel, M.R. Mehra, R.A. Schuepbach, F. Ruschitzka, H. Moch, Endothelial cell infection and endotheliitis in COVID-19, Lancet 395 (10234) (2020) 1417–1418, https://doi.org/10.1016/S0140-6736(20)30937-5.
[39] G.B. Danzi, M. Loffi, G. Galeazzi, E. Gherbesi, Acute pulmonary embolism and COVID-19 pneumonia: A random association? Eur. Heart J. 41 (19) (2020) https://doi.org/10.1093/eurheartj/ehaa254, 1858–1858.
[40] A. Jain, D.J. Doyle, R. Mangal, Mosaic perfusion pattern" on dual-energy CT in COVID-19 pneumonia: pulmonary vasoplegia or vasoconstriction? Radiol Cardiothorac Imaging 2 (5) (2020) https://doi.org/10.1148/ryct.2020200433.
[41] S. Si-Mohamed, N. Chebib, M. Sigovan, L. Zumbihl, S. Turquier, S. Boccalini, L. Boussel, J.F. Mornex, V. Cottin, P. Douek, In vivo demonstration of pulmonary microvascular involvement in COVID-19 using dual-energy computed tomography, Eur. Respir. J. 56 (2020), 2002608, https://doi.org/10.1183/13993003.02608-2020.
[42] G.E. Antonio, K.T. Wong, D.S. Hui, A. Wu, N. Lee, E.H. Yuen, C.B. Leung, T. H. Rainer, P. Cameron, S.S. Chung, J.J. Sung, A.T. Ahuja, Thin-section CT in patients with severe acute respiratory syndrome following hospital discharge: preliminary experience, Radiology 228 (September 3) (2003) 810–815, https://doi.org/10.1148/radiol.2283030726. Epub 2003 Jun 12. PMID: 12805557.
[43] N. Chen, M. Zhou, X. Dong, J. Qu, F. Gong, Y. Han, Y. Qiu, J. Wang, Y. Liu, Y. Wei, J. Xia, T. Yu, X. Zhang, L. Zhang, Epidemiological and clinical characteristics of 99 cases of 2019 novel coronavirus pneumonia in Wuhan, China: a descriptive study, Lancet. 395 (10223) (2020) 507–513, https://doi.org/10.1016/S0140-6736(20)30211-7.
[44] K.W. Choi, T.N. Chau, O. Tsang, E. Tso, M.C. Chiu, W.L. Tong, P.O. Lee, T.K. Ng, W. F. Ng, K.C. Lee, W. Lam, W.C. Yu, J.Y. Lai, S.T. Lai, Princess margaret hospital SARS study group. Outcomes and prognostic factors in 267 patients with severe acute respiratory syndrome in Hong Kong, Ann. Intern. Med. 139 (9) (2003) 715–723, https://doi.org/10.7326/0003-4819-139-9-200311040-00005.